Catal Lett (2012) 142:521–530
DOI 10.1007/s10562-012-0804-6

Molybdenum Oxoanions as Dispersing Agents in the Preparation of Pd/C Catalysts for the Selective Oxidation of Glyoxal

S. Hermans · F. Thiltges · A. Deffernez · M. Devillers

Received: 21 October 2011 / Accepted: 11 March 2012 / Published online: 27 March 2012

Abstract Catalysts Pd/C were prepared in the presence of Mo oxoanions. The size of Mo precursor and the electrostatic interactions with the Pd precursor during the synthesis were found to be responsible for high Pd dispersions. These catalysts were very active for glyoxal oxidation into glyoxalic acid.

Keywords Carbon · Palladium · Molybdenum · Glyoxal · Glyoxalic acid · Selective oxidation · Heteropolyanion

1 Introduction

Polyoxometallates (POMs) and related inorganic metal–oxygen cluster compounds are intensely studied because of their rich chemistry and variable structures [1, 2]. They are amenable to covalent organic functionalization [3, 4], and modification by thermal treatment [5] or pH variations. This versatility has opened doors for applications in analytical chemistry, materials science, biochemistry, medicine and geochemistry. In catalysis, it is their redox and acido-basic properties that are exploited for applications [6–10]. They are used for example as oxidation catalysts in liquid phase [11–13], with the possibility of catalyzing multi-electron redox reactions. The so-called heteropolyacids (HPAs) are used as strong inorganic acids in various catalytic processes [14, 15], in solution or as solid acid catalysts [7]. HPAs can also be supported to be applied in acid [16–18] or oxidation heterogeneous catalysis [12].

S. Hermans (✉) · F. Thiltges · A. Deffernez · M. Devillers
Institute of Condensed Matter and Nanosciences (IMCN), Université catholique de Louvain, Place Louis Pasteur, 1/3, 1348 Louvain-la-Neuve, Belgium
e-mail: Sophie.Hermans@uclouvain.be

In this context, the interaction between POMs, and HPAs in particular, with various surfaces has been studied extensively. It has been shown in many instances that their anionic character allows ion-pairing with charged surface sites or ion-exchange. A solid-state NMR study has shown that HPAs interact strongly with carbon [19]. The interaction of W-based HPAs and filamentous carbon has also been studied [20]. Another study demonstrated that HPAs interact more strongly with carbon than with silica [21]. Phosphomolybdic acid ($H_3PMo_{12}O_{40}$) has even been used as inorganic surfactant for carbon-black suspensions, thanks to its strong chemisorption on carbon surfaces [22]. The interaction between anionic Mo species and carbon supports modified by oxidation has also been investigated [23]. Carbon-supported HPAs have been applied as catalysts for liquid-phase oxidation and esterification, because of their stability toward HPA leaching from the carrier [8, 24, 25]. Pd nanoparticles supported on phosphomolybdic acid–poly(diallyldimethylammonium chloride) functionalized multiwalled carbon nanotubes have also been demonstrated to be superior electrocatalysts [26].

We have shown that the so-called 'Strong Electrostatic Absorption' (SEA) method developed by Regalbuto et al. [27] has its limits for depositing Pd(II) on carbon, because the large pH-window for maximum surface absorption corresponds to the existence of neutral Pd species in solution, thus precluding an electrostatic mechanism from taking place [28–30]. The goal of the present study is to take advantage of the charged nature of Mo POMs to interact electrostatically with the surface and serve as intermediate for the adsorption of Pd on carbon, for catalytic application in glyoxal selective oxidation. The risk of contaminating the final Pd/C catalyst by Mo can be taken given a report on Mo–Pt/C (claimed to be bimetallic) catalysts that are more active for the targeted transformation than the

corresponding Pt/C system [31]. Supported Mo–Pd catalysts have also been applied to other reactions [32–42]. In addition, although in the first paper describing heterogeneous catalysts for glyoxal oxidation, Pt/C catalysts were shown to be more active than Pd/C [43], we have since shown that main-group element-promoted E–Pd/C catalysts (E = Pb, Bi) are more active and selective than monometallic formulations [44–46]. However, the drawback of these bimetallic materials resides in the non-negligible leaching of the main group promoter element during catalyst' use. In consequence, we have been looking for alternative promoters for this reaction, which would not leach, but maintain the required high selectivity and activity. Ruthenium and gold were found to be promising candidates [29, 30, 47, 48], but the former had a mitigate action that seemed to be highly dependent on the preparation procedure, while the latter did not solve the economical constraint.

Glyoxal selective oxidation is a reaction of interest for several reasons. First, the variety of possible by-products (Fig. 1) makes it a challenge for the chemist. Controlling the selectivity towards the product of interest (glyoxalic acid) requires a fine balance at the catalyst' level. Second, selective oxidations carried out in water present a viable route for the valorization of renewable feedstocks. Finally, glyoxalic acid is an intermediate in a variety of pharmaceutical, cosmetic and food processes, such as vanillin synthesis [49].

2 Experimental

The support used for the preparation of catalysts was an SXplus active carbon (noted SX+; $S_{BET} \cong 800\ m^2/g$; particles sizes: 50–100 μm) supplied by Norit. The metallic precursors were palladium (II) acetate ($Pd(OAc)_2$, Rocc Pd: 47.27 %) or palladium(II) chloride ($PdCl_2$, Aldrich 99.9+ %) for Pd, and phosphomolybdic acid ($H_3PMo_{12}O_{40}$, Aldrich, abbreviated PM) or ammonium heptamolybdate ($(NH_4)_6Mo_7O_{24}.4H_2O$, Acros p.a., abbreviated AHM) for Mo. In one case, a W precursor analogous to phosphomolybdic acid was used ($H_3PW_{12}O_{40}$, Acros p.a.). Unless otherwise stated, the amounts of carbon and precursor(s) engaged in the preparations were calculated so as to correspond to a Pd loading of 5 wt% in the activated catalysts, and a Mo/Pd wt ratio (or W/Pd wt ratio) of 1/1. Three different preparation methods were used. In procedure **A**, the carbon support was suspended in water before adding the precursors in solution. The suspension was stirred, heated at 80 °C, before adding NaOH and formalin (formaldehyde 37 wt% in water, Aldrich) for activation. In procedure **B**, the carbon support and the Pd precursor were first suspended in *n*-heptane (Acros, 99+ %) and sonicated, followed by slow evaporation of the solvent. This monometallic non-activated catalyst was then introduced in suspension in water, to which an aqueous solution of the Mo precursor was added, before stirring overnight, heating

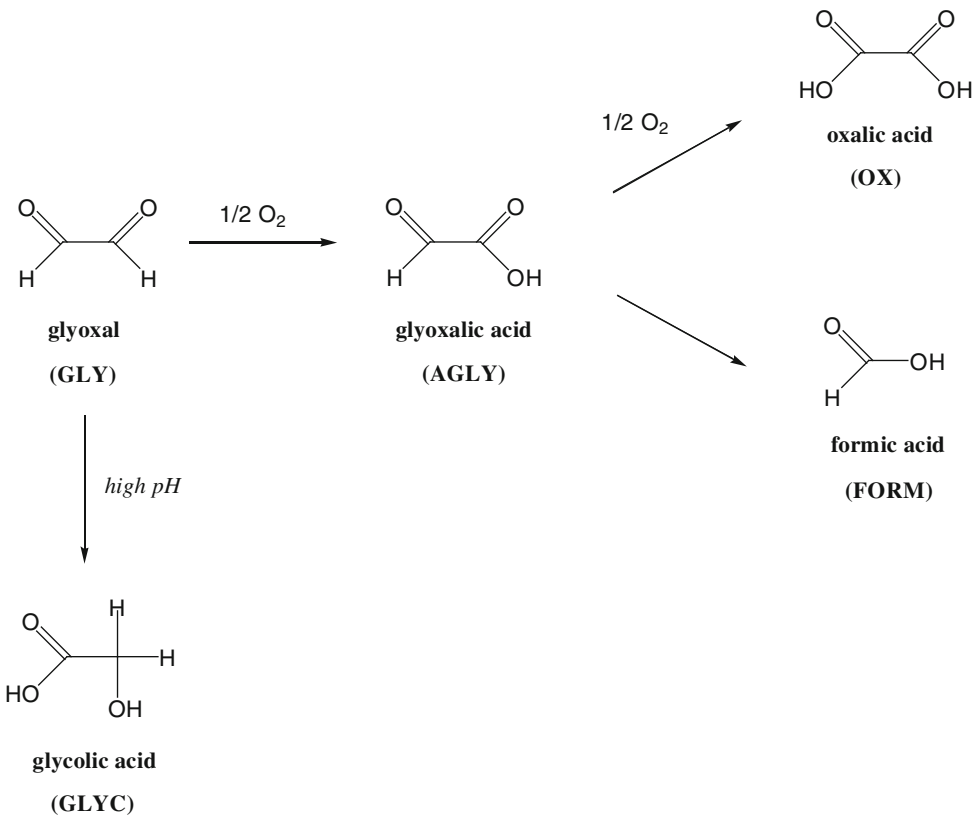

Fig. 1 Possible products arising from glyoxal oxidation

at 80 °C, adding NaOH and formalin for activation. In a slight modification of this method (called **B**'), Pd was brought into contact with the carbon support in benzene solution, because it gave previously good results for the preparation of Pd/C catalysts from carboxylate-type precursors for glucose oxidation [50]. In procedure **C**, the monometallic non-activated catalyst prepared in *n*-heptane is re-introduced in the same solvent in the presence of the Mo precursor, sonicated again, before slow evaporation and activation at 500 °C for 18 h under N_2 flow in a tubular oven. A variation (called **C**') implies a procedure similar to **C**, but with an additional formalin activation step after thermal treatment. In all cases implying aqueous suspensions, the filtrates of the syntheses were analyzed by atomic absorption, using a Perkin-Elmer 3110 spectrometer, in order to determine the residual amounts of metals that were not adsorbed on the support.

The catalysts were tested for glyoxal oxidation in a double-walled glass reactor, as previously described [44–46]. The temperature was fixed at 38 °C by water circulation in the outer compartment, and a mechanical stirrer (Heidolph RZR 2051) ensured a constant stirring rate of 1,000 rpm. The acids formed were continuously neutralized by addition of Na_2CO_3 0.3 mol/L (Merck), thanks to an automatic titration device Stat Titrino 718 from Metrohm, equipped with a combined electrode Beckman 39843, which allowed the pH to be fixed at a constant value of 7.2 ± 0.5. The tests were carried out with 400 ml of glyoxal (0.1 mol/L solution, Acros), 100 mg of catalyst, and an air flow of 0.4 L/min as oxidant. Standard tests have been performed to ensure that mass transfer limitations can be ruled out, using either half mass of catalyst or higher stirring speed. Each catalyst has been tested 2–3 times, and the results presented here have been averaged. When a detailed analysis of the products distribution over time has been carried out, 0.5 mL samples of the reaction mixture were taken at regular intervals and the results were corrected for volume variations.

The products formed were quantified by HPLC (liquid chromatograph TSP Spectra Series P200), on an Aminex BioRad HPX-87H column, heated at 60 °C, and using sulfuric acid (solution 0.005 mol/L) as eluent (flow rate: 0.4 mL/min). The products were detected at 230 nm on a TSP Spectra System UV6000LP diode array detector, and the quantification was possible after calibration with standard solutions. The reaction mixtures were also analyzed by atomic absorption (after removal of the catalyst by filtration), and by ICP-AES, using a Perkin-Elmer Optima 3000 SC apparatus, in order to detect metal leaching (if any) during catalyst use.

The catalytic results are expressed in terms of yield in each product (Y, %, see Fig. 1 for abbreviations used), conversion (X, %) and selectivity (S, %), defined as follows:

$$Y = C_{PRODUCT}/C_{GLY\,at\,t=0}\ where\ C = concentration \quad (1)$$

$$X_{GLY} = Y_{AGLY} + Y_{OX} + Y_{GLYC} + (Y_{FORM}/2) \quad (2)$$

$$S_{AGLY} = (Y_{AGLY}/X_{GLY}) \times 100 \quad (3)$$

when the yield in glycolic acid is neglected (because its formation does not depend on the catalyst but only on the pH, by Cannizzaro dismutation), a 'corrected' conversion (X^*, %) and a 'corrected' selectivity (S^*, %) are quoted, following:

$$X*_{GLY} = Y_{AGLY} + Y_{OX} + (Y_{FORM}/2) \quad (4)$$

$$S*_{AGLY} = (Y_{AGLY}/X*_{GLY}) \times 100. \quad (5)$$

The solid catalysts were characterized by X-ray photoelectron spectroscopy (XPS), X-ray powder diffraction (XRD), scanning electron microscopy (SEM), and CO chemisorption. The XPS measurements were carried out on a SSI-X-probe (SSX-100/206) photoelectron spectrometer from Surface Science Instruments (USA) equipped with a monochromatized microfocus Al X-ray source. The samples were stuck onto small troughs with double-sided adhesive tape, and then placed on an insulating home-made ceramic sample stage (Macor® Switzerland). A flood gun set at 8 eV and a Ni grid placed 3 mm above the samples surface were used to avoid differential charging effects. The quantification was based on the C1s, Pd3d, Mo3d, Cl2p, P2p and Na1s photopeaks. The energy calibration was done with reference to the peak $Au4f_{7/2}$ at 84 eV, and the binding energies were calculated with respect to the C–(C, H) component of the C1s peak fixed at 284.8 eV. Data treatment was performed with the CasaXPS program (Casa Software Ltd., UK). The spectra were decomposed with the least squares fitting routine provided by the software with a Gaussian/Lorentzian (85/15) product function, after subtraction of a Shirley type baseline, and using the following constraints for palladium and molybdenum, respectively: intensity ratio ($Pd3d_{5/2}/Pd3d_{3/2}$) = 1.5, Δ = 5.26 eV, FWHM ratio = 1; intensity ratio ($Mo3d_{5/2}/Mo3d_{3/2}$) = 1.5, Δ = 3.13 eV, FWHM ratio = 1. The XRD analyses were performed with a D-5000 SIEMENS diffractometer equipped with a copper source ($\lambda_{K\alpha}$ = 154.18 pm). The samples were supported on quartz monocrystals, and the phases detected were identified by reference to the JCPDS-ICDD database. SEM analyses were performed on a field effect gun digital scanning electron microscope (DSM 982 Gemini from LEO), equipped with an energy dispersive X-ray system (EDAX Phoenix equipped with a CDU LEAP detector). The powder samples were pressed onto conducting double-face adhesive tape fixed onto 0.5" aluminium specimen stubs from Agar Scientific. The CO chemisorption

measurements were carried out on a Pulse Chemisorb 2700 apparatus from Micromeritics. The samples (~30 mg) were first submitted to a pretreatment at 150 °C under H_2 (30 mL/min) for 1 h, followed by 2 h at 200 °C under helium (30 mL/min). The analysis was conducted in pulse mode, by using repeatedly an injection volume of 50 μL CO, until saturation. The Pd dispersion was calculated from the sum of non-detected CO in each pulse, when compared to the saturation value, and by considering a surface Pd:CO stoichiometry equal to 1. Transmission electron microscope (TEM) images were obtained with a LEO 922 OMEGA energy filter TEM; the sample was suspended in diethylether and a drop of the supernatant was deposited on a holey carbon film supported on a copper grid. ICP-OES analysis was carried out by Medac Ltd. (UK).

3 Results and Discussion

Various catalysts were prepared by combining one of the palladium precursors ($Pd(OAc)_2$ or $PdCl_2$) with one of the molybdenum precursors (PM or AHM), and using one of the preparation methods described in the "Experimental" section part (Table 1). In each case, Pd and Mo precursors were adsorbed on the carbon support in excess solvent, followed by activation. The goal of the activation is to reduce Pd(II) species into Pd(0), and this was carried out either chemically by the action of the chemical reducing agent formaldehyde at basic pH (obtained by adding NaOH in the preceding step), or thermally by decomposition of the coordination compounds under nitrogen (spontaneous reduction of noble metal under inert atmosphere upon loss of ligand). The obtained materials were tested in glyoxal oxidation for 20 h, in order to identify the active combinations. The catalytic activity and selectivity were found to depend strongly on the nature of the precursors and on the preparation method used. The best catalyst combined PM as Mo precursor, $Pd(OAc)_2$ as Pd precursor, and procedure **B**. The results obtained were by far better than with reference monometallic Pd/C catalysts (Table 1), and compared very well with bimetallic Bi–Pd/C catalysts, whose performance were reported earlier [44–46]. The results obtained here are similar to Pd/C catalysts prepared by the optimized adsorption method [28], but obviously not as good (at t = 20 h) as the Au-promoted optimized Pd/C systems [29, 30]. A Pd-free catalyst prepared following the same procedure, but introducing only the Mo precursor, was checked to be completely inactive ($Y_{AGLY} < 1\%$). These results demonstrate that the use of Mo oxoanions during the preparation can play a positive role for the activity of Pd in this reaction. However, in some cases (see Table 1), the preparation of materials from Mo and Pd precursors led to catalytic results that were worse than with the Pd/C equivalents. The chemical activation step with formalin (procedure **A** or **B**) seems compulsory in order to produce active catalysts, while the thermal treatment (procedure **C**) is deleterious and cannot be compensated by subsequent formalin activation (procedure **C'**). In all cases, no traces of solubilized Pd were found in the reaction mixtures after tests (detection limit: 50 ppb). The activity of the best catalyst (PM as Mo precursor, $Pd(OAc)_2$ as Pd precursor, and synthetic procedure **B**) was studied as a function of time (Fig. 2). Given the complex reaction scheme (see Fig. 1), the yield in glyoxalic acid usually reaches a maximum (after a period of time that we call t_{max}, and which depends on the catalyst) before decreasing due to over-oxidation to oxalic acid. By contrast with previously reported results with Bi–Pd/C catalysts, where it had been identified at 24 h [45], the maximum yield in glyoxalic acid is here not yet attained after 48 h, but it is still in constant augmentation. The yield in glyoxalic acid obtained (after 48 h) is thus superior (or equal) to all former results obtained so far with the best catalysts for this reaction [28–30, 44–48]. This is particularly obvious when comparing the yields in glyoxalic acid normalized with respect to the amount of active metal (Pd) [28–30, 44–48],

Table 1 Catalytic results for the materials prepared from palladium ($Pd(OAc)_2$ or $PdCl_2$) and molybdenum (PM or AHM) precursors, at 20 h reaction time

Precursors used	Preparation method[a]	Y_{AGLY} (%)	Y_{OX} (%)	Y_{FORM} (%)	X^*_{GLY} (%)	S^*_{AGLY} (%)
$Pd(OAc)_2/C_{sx+}$	C	3.1	0	0.5	1.4	81.2
$PdCl_2/C_{sx+}$	A	1.3	0	0.4	1.5	84.0
$Mo(PM)Pd(OAc)_2/C_{sx+}$	B	15.1	2.9	5.1	20.9	71.9
$Mo(PM)Pd(OAc)_2/C_{sx+}$	C	0.3	0	0.1	0.3	81.3
$Mo(PM)Pd(OAc)_2/C_{sx+}$	C'	1.2	0	0.5	1.4	84.1
$Mo(PM)Pd(OAc)_2/C_{sx+}$	B'	8.9	1.1	2.5	11.2	79.3
$Mo(AHM)Pd(OAc)_2/C_{sx+}$	B	9.6	2.6	11.5	18.0	53.7
$Mo(PM)PdCl_2/C_{sx+}$	B	10.8	1.3	4.1	15.8	76.0
$Mo(AHM)PdCl_2/C_{sx+}$	B	3.9	0.3	3.1	49.1	67.5
$Mo(AHM)Pd(OAc)_2/C_{sx+}$	C	0.8	0	1.1	1.3	58.0

[a] See "Experimental" section part for details

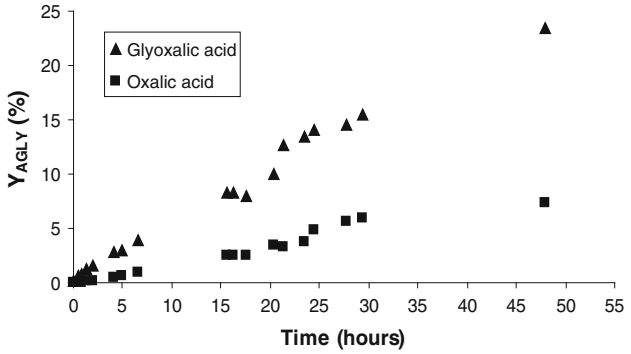

Fig. 2 Evolution over time of the yields in glyoxalic and oxalic acids for the catalyst prepared from PM as Mo precursor, $Pd(OAc)_2$ as Pd precursor, and following procedure **B**

i.e. $(\mathbf{Y_{AGLY}})_{max}$**/mPd** (mol/g): Bi–Pd/C (t_{max} = 24 h) **1.22**, Pd–Au/C (t_{max} = 24 h) **1.6–2.0**, Pd1Ru1/C (t_{max} > 72 h) **1.44**, here (t_{max} > 48 h) **1.9**.

The catalysts described above were characterized by XPS, and the results obtained are presented in Table 2. The first striking observation is that the catalysts prepared in the presence of PM or AHM do not contain any Mo on the surface in their final (activated) form. These catalysts should therefore not be considered as "bimetallic", but the effect of Mo on the catalysts' performance is real (when compared to the materials prepared in the absence of Mo precursor, see Table 1) and has to be explained in terms of a synthesis additive. In fact, as proven by atomic absorption analysis, Mo was recovered from the preparations filtrates, while no traces of Pd were detected. A second striking observation from Table 2 is that the most active catalysts display the highest experimental Pd/C ratios, a parameter that is linked to the metal dispersion and localization of Pd at the external surface. As the carbon support is microporous, this might be advantageous when carrying out catalysis in water. And finally, it is also obvious that the catalysts prepared in the presence of Mo display higher Pd/C ratios than their monometallic counterparts, indicating that the main effect of Mo is on this parameter. A further analysis of the XPS results shows that thermal activation leads to lower Pd/C ratios, hence lower activity, and that the catalysts before and after test present a similar surface state. The relationship between catalytic activity (Y_{AGLY}) and the Pd/C ratio determined by XPS is not linear, but, as shown in Fig. 3, it behaves as if there was a switch-value (Pd/C (×100) = 2) under which the activity is cancelled, and above which the catalyst functions effectively. Higher values of Pd/C ratios do not bring further improvement of the catalytic activity, perhaps due to an increased poisoning rate of the Pd surface by oxygen at very high dispersions [51].

To improve the understanding of these experimental features, the best catalyst (prepared via procedure **B**) has also been characterized by XPS at each step of its synthesis (Table 3). It was found that Mo *is present* on the carbon surface until NaOH is added, at which point most of it is lost. Once treated with formalin, the catalyst surface becomes completely Mo-free. Another very interesting observation is that the Pd/C ratio is rather low at the end of the first step in the synthesis (when the Pd precursor has been deposited on the carbon support from a suspension in *n*-heptane), but it increases dramatically once brought into contact with Mo in aqueous solution. The effect of the Mo precursor on this parameter related to Pd dispersion is thus unmistakable and immediate, and involves a surface phenomenon where Mo is present.

The best catalyst (prepared from PM and $Pd(OAc)_2$ via procedure **B**) was also characterized by XRD after activation. The diffractogram obtained did not display any peak, indicating that the particles of Pd in the catalyst were very small (under the minimal crystallite size detectable by XRD). This was confirmed by SEM (Fig. 4). The electron micrographs revealed a homogeneous distribution of

Table 2 XPS results for the materials prepared from palladium ($Pd(OAc)_2$ or $PdCl_2$) and molybdenum (PM or AHM) precursors

Precursors used	Preparation method[a]	Y_{AGLY} (%)	Mo/C (×100)			Pd/C (×100)		
			Calc.[b]	Exp.[c]		Calc.[b]	Exp.[c]	
				Before test	After test		Before test	After test
$Pd(OAc)_2/C_{sx+}$	B	0.4	–	–	–	0.59	0.79	0.81
$PdCl_2/C_{sx+}$	A	1.3	–	–	–	0.59	1.48	1.04
$Mo(PM)Pd(OAc)_2/C_{sx+}$	B	15.1	0.62	0	0	0.62	3.47	4.09
$Mo(PM)Pd(OAc)_2/C_{sx+}$	C	0.3	0.62	0	0	0.62	1.42	1.54
$Mo(PM)PdCl_2/C_{sx+}$	B	10.8	0.62	0	0	0.62	4.41	2.66
$Mo(AHM)Pd(OAc)_2/C_{sx+}$	B	9.6	0.62	0	0	0.62	3.92	3.74

[a] See "Experimental" part for details

[b] Calc. = values calculated from the bulk composition

[c] Exp. = experimental values retrieved from XPS data analysis

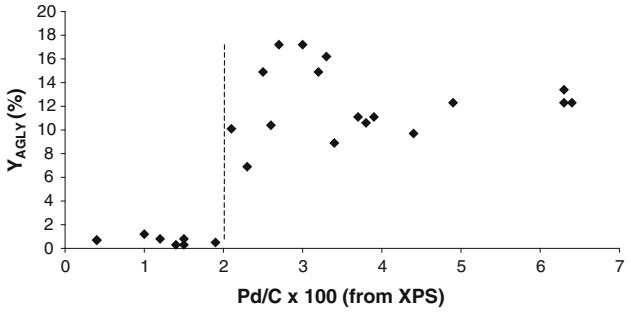

Fig. 3 Correlation between catalytic activity (yield in glyoxalic acid at 20 h reaction time) and XPS results (Pd/C surface atomic ratio $\times 100$)

particles of very small sizes (<10 nm) on the surface. Moreover, EDXS analysis showed the presence of only C and O (arising from the SX+ active carbon support with its oxygenated functions) together with Pd, confirming the absence of Mo observed by XPS. It was also imaged by TEM (Fig. 5) and indeed small particles 2–5 nm in size were observed, homogeneously distributed on the support and presenting a narrow size distribution. The dispersion of Pd in this catalyst was measured by CO chemisorption, and a value of 17.5 % was obtained. The solid sample was analyzed by ICP-OES which gave a bulk mass percentage of Pd 4.63 and Mo 0.18 wt% in the catalyst. This is consistent with the nominal value of 5 wt% Pd and the absence of Mo observed by XPS (within experimental error). The very small amount of Mo present (0.18 wt% rather than 5 wt% engaged) could of course be responsible for some promoter action during catalysis, but we believe this not to be the major effect. Using the same preparation procedure, a monometallic Mo/C catalyst was prepared, which was found inactive ($Y_{AGLY} < 1$ %) as mentioned above. In addition, a catalytic test was carried out with a monometallic Pd/C catalyst prepared by the same procedure, in the presence of phosphomolybdic acid (in 1:1 wt ratio with respect to Pd in the catalyst) in solution. Again, no significant rise in activity was found. Another experiment with five-fold excess of phosphomolybdic acid in solution gave the same result.

In order to understand the positive role that Mo plays on the Pd dispersion, a series of additional experiments were carried out. First, given that PM is a strong acid, the synthesis of Pd (5 wt%)/C catalysts was carried out (following procedure **B**) in the presence of nitric or phosphoric acid, in order to reach a similar pH during the preparation but without any Mo in solution (pH = 1.85). In both cases, the catalytic activity was cancelled ($Y_{AGLY} < 2$ %), indicating that the effect of Mo is not only due to the acidic character of its precursor. XRD characterization of the catalyst prepared in the presence of H_3PO_4 showed small peaks attributable to Pd, indicating the presence of small crystallites of palladium on the carbon surface (while no peak was detected in the case of the best Pd/C catalyst prepared in the presence of Mo, see above). The Pd/C ratio ($\times 100$) obtained by XPS for this material was 0.55, while SEM images of the sample (Fig. 6a) showed an inhomogeneous distribution of metal particles, with small particles (<50 nm) coexisting with bigger aggregates (up to 1 μm). Moreover, the EDXS analysis (Fig. 6b) showed the presence of C and O (from the support), together with Pd, as expected, but also residual P and Cl, which might have a poisoning effect on the catalytic activity. In a second experiment, phosphomolybdic acid was replaced-in procedure **B**—by the equivalent amount of phosphotungstic acid ($H_3PW_{12}O_{40}$). In this case, the catalytic activity was retained: $Y_{AGLY} = 13.4$ %, to compare with 15.1 % in the case of Mo (Table 1), indicating that the nature of the metal in the synthesis additive is not the crucial factor either. The Pd/C ratio measured by XPS was also high (Pd/C ($\times 100$) = 6.32), which points towards a similar mechanism of action, based on a dispersion increase. Finally, given that the PM precursor is a heteropolyanion with a Keggin structure, a synthesis in the presence of a monomeric molybdate, i.e. $(NH_4)_2MoO_4$ at pH > 8, was envisaged. When comparing the two Mo precursors (PM comprising 12 Mo and AHM comprising 7 Mo atoms) with the "monomer", in the same preparation method (**B**), a gradual decrease of the catalytic activity (Y_{AGLY}) was observed, from 15.1 % with PM, to 9.6 % with AHM, down to <1 % with $(NH_4)_2MoO_4$, suggesting that the *size* of the Mo precursor is an important factor (rather than merely the pH of the solution).

Table 3 XPS results at each step of the synthesis using procedure **B**, with $Pd(OAc)_2$ and PM as precursors

Synthetic step	Pd/C ($\times 100$)	Mo/C ($\times 100$)	Pd(II)/Pd(0)
1. After deposition of the Pd precursor in *n*-heptane	0.78	0.0	0.61
2. After suspension in water and addition of PM + 1 h stirring	2.27	0.69	0.75
3. After 6 h stirring	5.39	1.09	2.75
4. After 15 h stirring	4.15	1.43	0.89
5. After addition of NaOH	5.90	0.19	5.99
6. After addition of formalin	3.51	0.0	0.46

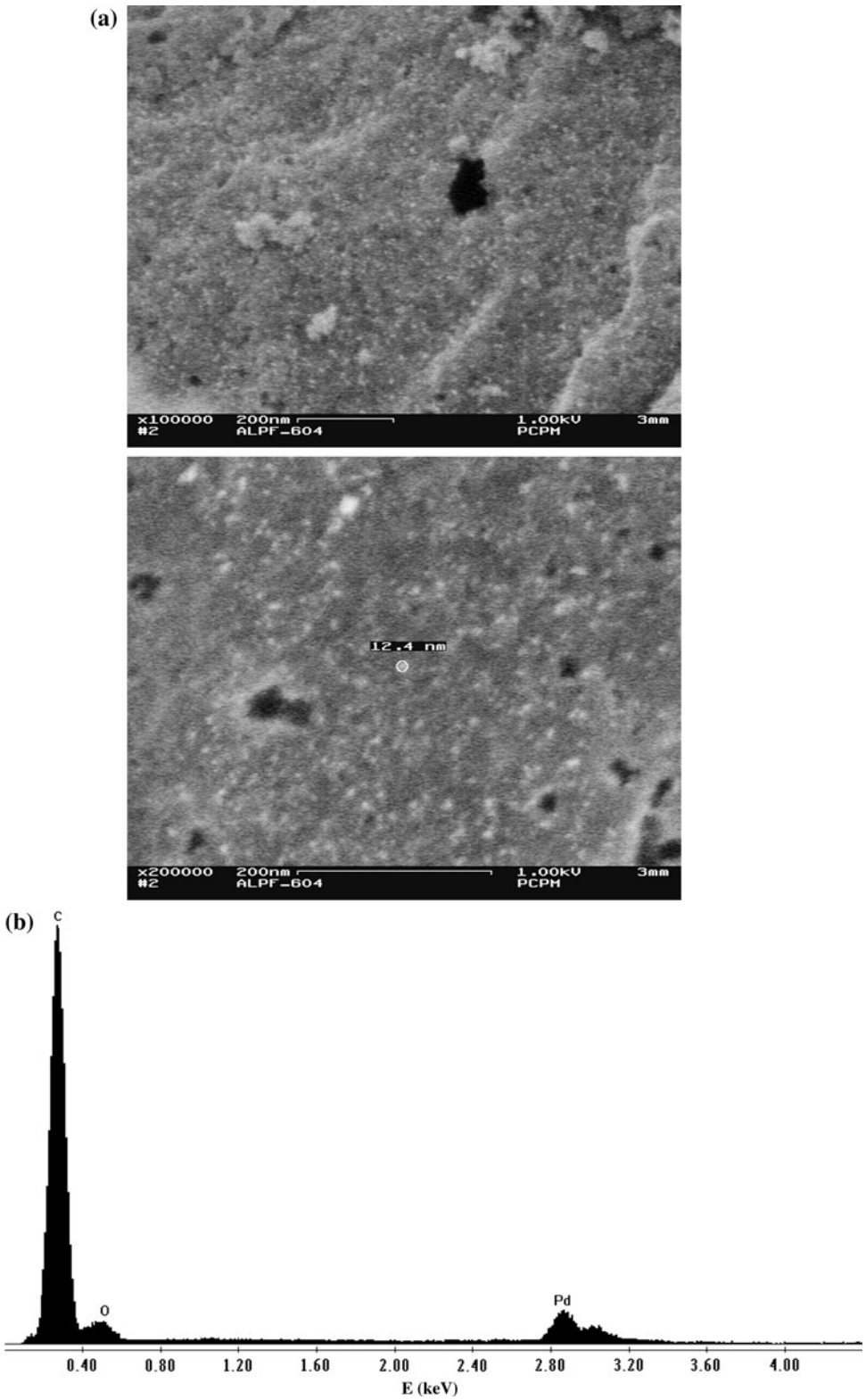

Fig. 4 **a** SEM images obtained for the best catalyst (prepared from PM and $Pd(OAc)_2$ via procedure **B**), and **b** representative EDXS spectrum obtained for this sample

This allows us to envision the mechanism of action of Mo for the preparation of highly active Pd/C catalysts as follows. First of all, when $Pd(OAc)_2$ is deposited on carbon from *n*-heptane, it is still probably in trimeric form, as in the solid state, because it is insoluble in this medium. Secondly, when this material is suspended in aqueous solution, which is acidic in nature because of the presence of the Mo precursor (pH = 1.85), Pd can be assumed to

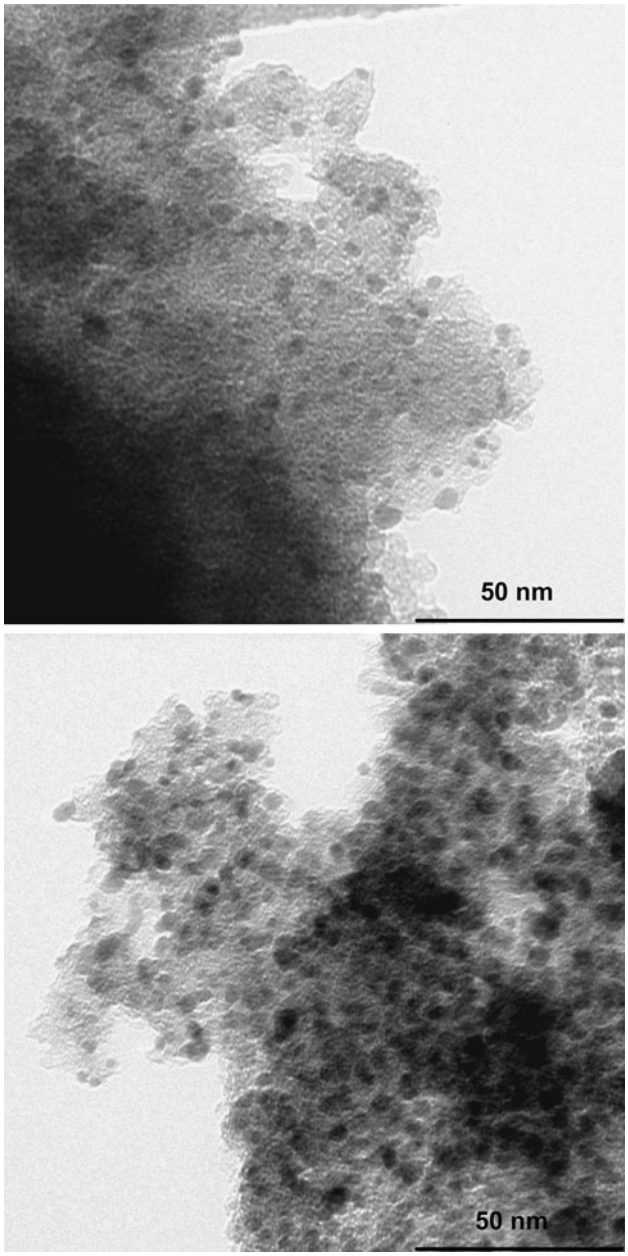

Fig. 5 TEM images obtained for the best catalyst (prepared from PM and $Pd(OAc)_2$ via procedure **B**)

exchange its acetate ligands for H_2O molecules and be present essentially as its positively charged tetraaqua Pd(II) complex, $[Pd(H_2O)_4]^{2+}$ [28]. The Mo precursor, being a strong acid, is anionic in aqueous solution ($[PMo_{12}O_{40}]^{3-}$). The presence of Mo leads to a Pd dispersion increase: this must be due to an interaction between Pd(II) and PM, and between those and the carbon surface. The interaction between Pd(II) and PM would be electrostatic and easily understood from the fact that they bear opposite charges. Interactions of Pd(II) with $H_3PMo_{12}O_{40}$ in solution were studied and identified as aqua-or hydroxo palladium complexes adsorbed on the polyanion surface [52]. The interaction with the support might be maximized thanks to the presence of the Mo species, as it is known that polyoxometalates get adsorbed strongly on carbon surfaces [19, 21, 24, 53]. It has been quoted that this strong interaction is mediated by the nitrogen or oxygenated surface groups of activated carbon [24, 54–56]. A study of the adsorption of $(NH_4)_6Mo_7O_{24}$ as a function of pH (going from pH = 9–2) on high surface area activated carbon has also shown that interaction with surface O-groups play a role in the adsorption of Mo species but that an electrostatic mechanism could happen within certain pH values [57]. Here, at low pH values, the C_{SX+} surface is positively charged, being below both IEP and PZC values. An electrostatic repulsion between C_{SX+} and $[Pd(H_2O)_4]^{2+}$ has been observed below pH = 2 [28], so the anionic Mo precursor would play the role of intermediate (electrostatic "glue"). Thirdly, as the size of the Mo precursor matters, but not the nature of the metal (Mo can be replaced by W and still play its role), there must be a steric effect. This can be seen as a "spacer" effect: the bigger the Mo precursor, the larger the distance between Pd atoms, and the lesser the trend towards agglomeration. This would explain higher Pd dispersion, hence higher catalytic activity. Finally, when NaOH is added, the Mo precursor probably looses its structure by a series of equilibriums due to the basicity of the pH (depolymerization of the heteropolyanion towards molybdate species), and desorbs because of a less perfect charge match (the pH being now above IEP and PZC values, causing the surface to be negatively charged). The palladium species might also precipitate because of the presence of OH^- ligands that enter the coordination sphere, replacing H_2O and forming neutral species of Pd(II). After reduction of Pd(II) into Pd(0) with formalin, the ion association at the surface cannot survive, hence the remaining Mo is desorbed. But the memory of the dispersing effect remains, and, at the end of the preparation procedure, Pd is present as very small metallic particles homogeneously dispersed on the support, which give high catalytic activity.

4 Conclusion

In this paper, we have shown that monometallic Pd/C catalysts can be prepared in the presence of Mo oxoanions, and give catalytic activities for the selective oxidation of glyoxal into glyoxalic acid that outnumber results obtained previously with promoted catalysts. The mechanism of action of the Mo species during the synthesis of these catalysts was studied, and it was found that it played the role of a dispersing agent. More precisely, a steric effect, forcing a homogeneous distribution of Pd(II) species on the support surface, was identified, and explained via

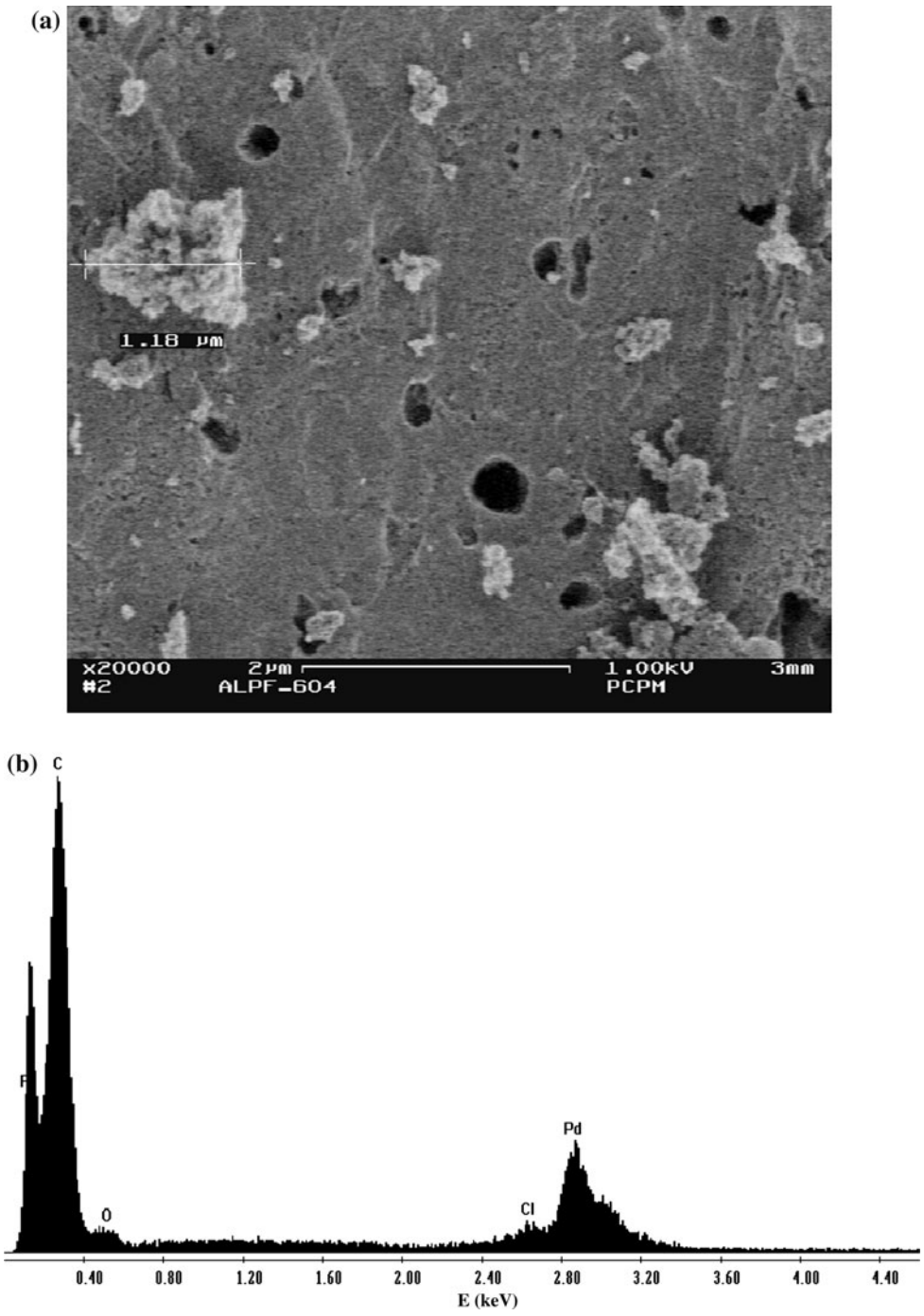

Fig. 6 **a** SEM image obtained for a catalyst prepared from $Pd(OAc)_2$ via procedure **B** in the presence of H_3PO_4 rather than *PM*, and **b** representative EDXS spectrum obtained for this sample

electrostatic interactions between the Pd and Mo precursors. At the end of the synthesis, Mo is completely desorbed from the surface, and the superior catalytic activity is not the result of a 'classical' synergetic effect as observed commonly in bimetallic heterogeneous catalysts, but of a high dispersion of Pd.

Acknowledgments The authors gratefully acknowledge financial support from the Belgian National Fund for Scientific Research (FNRS, Brussels) and the "Communauté Française de Belgique" (Concerted Research Programme). They also wish to thank G. Ploegaerts and V. Dubois (Institut Meurice, Brussels) for ICP and chemisorption measurements, J. -F. Statsijns for technical assistance, and the NORIT firm for supplying the carbon support.

References

1. Pope MT, Muller A (1991) Angew Chem Int Ed Engl 30:34
2. Jeannin YP (1998) Chem Rev 98:51
3. Gouzerh P, Proust A (1998) Chem Rev 98:77

4. Dolbecq A, Dumas E, Mayer CR, Mialane P (2010) Chem Rev 110:6009
5. Mestl G, Ilkenhans T, Spielbauer D, Dieterle M, Timpe O, Kröhnert J, Jentoft F, Knözinger H, Schlögl R (2001) Appl Catal A 210:13
6. Okuhara T, Mizuno N, Misono M (1996) Adv Catal 41:113
7. Mizuno N, Misono M (1998) Chem Rev 98:199
8. Kozhevnikov IV (1998) Chem Rev 98:171
9. Fawang C, Changwen H (2011) Prog Chem 23:19
10. Putaj P, Lefebvre F (2011) Coord Chem Rev 255:1642
11. Xianjun L, Ruiling L, Zhen L, Chungu X (2008) Prog Chem 20:469
12. Mizuno N, Kamata K, Yamaguchi K (2010) Top Catal 53:876
13. Matveev KI, Odyakov VF, Zhizhina EG (1996) J Mol Catal A 114:151
14. Corma A (1995) Chem Rev 95:559
15. Ueda T, Kotsuki H (2008) Heterocycles 76:73
16. Rocchiccioli-Deltcheff C, Aouissi A, Launay S, Fournier M (1996) J Mol Catal A 114:331
17. Bardin BB, Davis RJ (2000) Appl Catal A 200:219
18. Rives A, Payen E, Hubaut R, Vázquez P, Pizzio L, Cáceres C, Blanco M (2001) Catal Lett 71:193
19. Kozhevnikov IV, Sinnema A, Jansen RJJ, van Bekkum H (1994) Catal Lett 27:187
20. Timofeeva MN, Matrosova MM, Reshetenko TV, Avdeeva LB, Budneva AA, Ayupov AB, Paukshtis EA, Chuvilin AL, Volodin AV, Likholobov VA (2004) J Mol Catal A 211:131
21. Pizzio LR, Vázquez PG, Cáceres CV, Blanco MN (2003) Appl Catal A 256:125
22. Garrigue P, Delville M-H, Labrugère C, Cloutet E, Kulesza PJ, Morand J-P, Kuhn A (2004) Chem Mater 16:2984
23. Solar JM, Derbyshire FJ, de Beer VHJ, Radovic LR (1991) J Catal 129:330
24. Timofeeva MN, Matrosova MM, Il'inich GN, Reshetenko TV, Avdeeva LB, Kvon RI, Chuvilin AL, Budneva AA, Paukshtis EA, Likholobov VA (2003) Kinet Catal 44:778
25. Gall RD, Hill CL, Walker JE (1996) Chem Mater 8:2523
26. Cui Z, Kulesza PJ, Li CM, Xing W, Jiang SP (2011) Int J Hydrogen Energy 36:8508
27. Regalbuto JR (2009) In: de Jong KP (ed) Synthesis of solid catalysts. Wiley-VCH, Weinheim
28. Deffernez A, Hermans S, Devillers M (2007) J Phys Chem C 111:9448
29. Hermans S, Deffernez A, Devillers M (2010) Catal Today 157:77
30. Hermans S, Deffernez A, Devillers M (2011) Appl Catal A 395:19
31. Burmeister R, Deller K, Despeyroux B, Hatte C (1994) Patent no. EP635472-A, DE 43 24 442 C1
32. Da Silveira RS, De Oliveira AM, Pergher SBC, Da Silva VT, Baibich IM (2009) Catal Lett 129:259
33. Consul JMD, Costilla I, Gigola CE, Baibich IM (2008) Appl Catal A 339:151
34. Fernandez MB, Piqueras CM, Tonetto GM, Crapiste G, Damiani DE (2005) J Mol Catal A 233:133
35. Zina MS, Ghorbel A (2004) Solid State Sci 6:973
36. Pawelec B, Navarro RM, Campos-Martin JM, Agudo AL, Vasudevan PT, Fierro JLG (2003) Catal Today 86:73
37. Tonetto GM, Damiani DE (2003) J Mol Catal A 202:289
38. Sica AM, Baibich IM, Gigola CE (2003) J Mol Catal A 195:225
39. Li ZR, Fu YL, Jiang M, Meng M, Xie YN, Hu TD, Liu T (2000) Catal Lett 65:43
40. Noronha FB, Baldanza MAS, Schmal M (1999) J Catal 188:270
41. Konopny LW, Juan A, Damiani DE (1998) Appl Catal B Environ 15:115
42. Pavlova SN, Maksimovskaya RI, Kuznetsova LI (1991) Kinet Catal 32:361
43. Gallezot P, de Mésanstourne R, Christidis Y, Mattioda G, Schouteeten A (1992) J Catal 133:479
44. Alardin F, Delmon B, Ruiz P, Devillers M (2000) Catal Today 61:255
45. Alardin F, Ruiz P, Delmon B, Devillers M (2001) Appl Catal A 215:125
46. Alardin F, Wullens H, Hermans S, Devillers M (2005) J Mol Catal A 225:79
47. Hermans S, Devillers M (2005) Catal Lett 99:55
48. Deffernez A, Hermans S, Devillers M (2005) Appl Catal A 282:303
49. Mattioda G, Christidis Y (1989) Ullmann's encyclopedia of industrial chemistry, 5th ed., vol. A 12. VCH, Weinheim, p 495
50. Hermans S, Wenkin M, Devillers M (1998) J Mol Catal A 136:59
51. Besson M, Gallezot P (2000) Catal Today 57:127
52. Detusheva LG, Kuznetsova LI, Fedotov MA, Dovlitova LS, Vlasov AA, Likholobov VA, Malakhov VV (2003) Russ J Inorg Chem 48:1685
53. Schweglerl MA, Vinke P, van der Eijk M, van Bekkum H (1992) Appl Catal A 80:41
54. Jansen RJJ, van Veldhuizen HM, van Bekkum H (1996) J Mol Catal A 107:241
55. de la Puente G, Centeno A, Gil A, Grange P (1998) J Colloid Interface Sci 202:155
56. Martin Gullon A, Prado Burguete C, Rodriguez Reinoso F (1993) Carbon 31:1099
57. Rondon S, Wilkinson WR, Proctor A, Houalla M, Hercules DM (1995) J Phys Chem 99:16709